https://doi.org/10.30799/jnst.108.18040301 J. Nanosci. Tech. - Volume 4 Issue 3 (2018) 371–373

Share Your Innovations through JACS Directory

Journal of Nanoscience and Technology

Visit Journal at http://www.jacsdirectory.com/jnst

ISSN: 2455-0191

Metallic 1T Phase MoS_2 Nanosheets for Supercapacitor Application

K.M. Sarode, D.R. Patil*

Nanomaterial Research Laboratory, R.C. Patel Arts, Commerce and Science College, Shirpur – 425 405, Maharashtra, India.

ARTICLE DETAILS

Article history:
Received 09 April 2018
Accepted 17 April 2018
Available online 02 May 2018

Keywords:
MoS_2 Nanosheets
Electrode Materials
Supercapacitor

ABSTRACT

In the present study, a molybdenum disulfide MoS_2 nanosheets (MoS_2 NSs) were synthesized via a lithium intercalation and exfoliation method. The morphology and structure of the as-prepared MoS_2 was characterized by field emission scanning electron microscopy (FESEM), X-ray diffraction (XRD) and Raman spectrometer. The MoS_2 NSs electrode exhibited higher specific capacitance (148 Fg^{-1} at 1 mVs^{-1} or 142 Fg^{-1} at 1 Ag^{-1}) with excellent cycling stability, compared with bulk MoS_2. The result shows that MoS_2 is a promising electrode material for electrochemical supercapacitor.

1. Introduction

Nowadays, stable and high-performance energy-storage device has been paid tremendous research interest with the enhancing requirement of sustainable energy [1-3]. Supercapacitor is an updated kind of energy storage device, which possesses multiple strengths including, long cycle life, excellent power density, environment friendly, fast charge/discharge rate and better safety [4-7]. However, to date, most commercial electrical double layer capacitors (EDLCs) employ carbonaceous materials with large surface areas as electrode materials. Furthermore, carbon materials have some other drawbacks, such as low energy density and instability in aqueous electrolyte [8–10]. Thus, a growing attention has been focused on the development of redox-active materials such as conducting polymers [11] and metal oxide [12, 13] for pseudocapacitors.

Two-dimensional transition-metal dichalcogenides (2D TMDs) such as MoS_2 have recently attracted worldwide attention in various fields, such as sodium-ion batteries [14], lithium-ion batteries [15-17], electrochemical capacitors (ECs) [18-21], solid lubricants [22, 23], and catalysts [24, 25] benefiting from their distinct chemical and structure properties. MoS_2 has

Layered structure consisting of covalently bonded S- Mo- S, separated by a relatively weak van der Waals gap [26, 27]. Hence, it is easy to peel MoS_2 layers from the bulk [28, 29]. Nevertheless, MoS_2 usually exhibits the extremely low conductivity between two adjacent Van der Waals bonded layers would significantly suppress their overall electrochemical performance [30]. To solve this problem, adjusting the microcosmic morphology or connecting with other materials is an effective way.

Herein, we synthesized MoS_2 NS by lithium intercalation and exfoliation method. The physical Property and electrochemical performance of the as-obtained MoS_2 NS are evaluated in detail. The MoS_2 NS based electrodes were found to deliver a capacitance of 148 Fg^{-1} at 1 mVs^{-1}or 142 Fg^{-1} at 1 Ag^{-1} with excellent long-term cycling stability over 1000 cycles in 1 M KCl. The result indicates that the MoS_2 NS can be served as a promising electrode material for electrochemical supercapacitor.

2. Experimental Methods

2.1 Synthesis of MoS_2 NSs

The MoS_2 NSs were prepared by lithium intercalation and exfoliation method [31]. In a typical synthesis, 1.0 g of bulk MoS_2 powder was dispersed in 10 mL of 1.6 M butyllithium solution in hexane in a flask filled with N_2 gas. The mixture was soaked at room temperature for 48 h, and the obtained $LixMoS_2$ was centrifuged and washed with hexane to remove excessive lithium and organic residues. Exfoliation was achieved by sonicating the $LixMoS_2$ slurry in DI water for 1 h. The obtained aqueous suspension of MoS_2 NSs was centrifuged at 3,000 rpm for 25 min to discard the precipitates, and the supernatant was again centrifuged at 8,000 rpm for 25 min. The mixture was re-dispersed in DI water and re-centrifuged for several times and dried at 60 °C in vacuum. Finally, black MoS_2 crystalline powder was obtained.

2.2 Material Characterization

The crystalline structures of bulk MoS_2 and MoS_2 NSs were characterized by X-ray diffraction (XRD) (EMPYREAN with Cu Ka radiation, l = 1.5418 Å). The morphology was observed by field emission scanning electron microscopy (FESEM, Zeiss/ Ultra 55). A Raman spectrometer (Renishaw inVia, excitation 514.5 nm) was also used to characterize the synthesized materials.

2.3 Electrochemical Characterization

All electrochemical measurements were tested in a conventional three-electrode system using an electrochemical workstation; 1M KCl solutions were used as the electrolyte. The working electrodes were prepared by mixing the as-prepared active material, acetylene black and polyvinylidene difluoride (PVDF) with a mass ratio of 8:1:1, followed by the addition of N-methylpyrrolidone (NMP) to form homogenous slurry. The obtained slurry was then coated onto a stainless-steel current collector (an exactly $1cm^2$ active area) and dried at 60 °C for 12 h. The electrochemical performance of the fabricated electrodes was characterized by cyclic voltammetry (CV), galvanostatic charge/discharge (GCD). The CV curves were recorded at various scan rates (1, 2, 5, 10, and 20 mVs^{-1}) in a potential window of -0.5 to 0.2 V. The GCD curves were obtained at various current densities (1, 2, 3, and 5 Ag^{-1}) in a potential window of -0.5 to 0.2 V

The specific supercapacitance of the as-prepared electrode was calculated from the cyclic voltammetry [Eq.(1)] and galvanostatic charge discharge curves [Eq.(2)], according to the following equations:[32]

$$C_s = \int I(V)dv / vm\Delta v \qquad (Fg^{-1}) \qquad (1)$$

$$C_m = I\Delta t / m\Delta V \qquad (Fg^{-1}) \qquad (2)$$

where Cs is the specific capacitance (Fg^{-1}), I (V) dv is the integrated area of the CV curve (AV), v is the scan rate (mVs^{-1}), m is the mass of the active material (g), ΔV is the potential window (V), I is the discharge current (A), and Δt is the discharge time (s).

*Corresponding Author:dr.drpatil@gmail.com(D.R. Patil)

https://doi.org/10.30799/jnst.108.18040301

3. Results and Discussion

3.1 Characterization of MoS_2 NS

Fig. 1 shows the FESEM images of the bulk MoS_2 and MoS_2 NSs. The bulk MoS_2 exhibited largely micrometer-sized inerratic nanosheets, which are tightly stacked. After lithiation-exfoliation, the morphology of MoS_2 NSs interestingly changed to highly scattered nanoflakes. It is also noted that the size and thickness of the nanosheets were significantly decreased relative to the bulk phase.

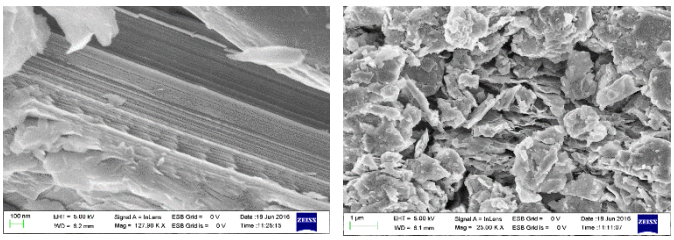

Fig. 1 FESEM images of (a) bulk MoS_2, (b) MoS_2 NS

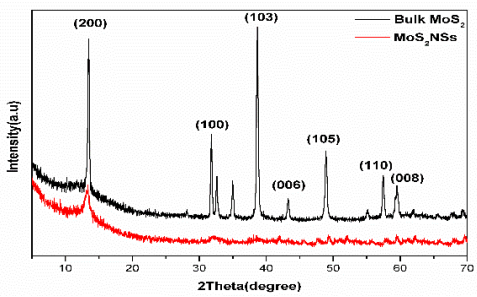

Fig. 2 X-ray diffraction patterns of bulk MoS_2 and MoS_2 NSs

Fig. 2 shows the XRD patterns of bulk MoS_2 and MoS_2 NSs. The diffraction peaks located at 2θ=14.4°, 33°, 38°, 48°, 58⁰ and 59° correspond to the planes of (002), (100), (103), (105), (110), and (008) respectively, agreeing well with the hexagonal phase of MoS_2 (JCPDS card no. 37-1492). After lithiation-exfoliation, a MoS_2 NSs show broadened peaks and lower peak intensity, indicating the crystallite size and the number of layers along the c axis are much smaller than those of bulk MoS_2 [33].

There are five distinct Raman scattering peaks for MoS_2 NSs prepared by lithiation-exfoliation method (Fig. 3). Among them, the peaks at 380.1 cm^{-1} and 402.4 cm^{-1} belong to the in-plane $E^1{}_2g$ and out-of-plane A_{1g} modes, respectively[34, 35]. Compared with bulk MoS_2, A_{1g} vibration softens, which indicates the MoS_2 NSs has small thickness [36]. Moreover, three relative weak peaks located at 153 cm^{-1} (I_1), 227 cm^{-1} (I_2), and 327 cm^{-1} (I_3) are not seen in bulk MoS_2, corresponding to the vibrations at the M points of the Brillouin zone [35]. The presence of I_1, I_2, and I_3 suggests that 1T MoS_2 exists in as-prepared MoS_2 NSs, because these vibrational modes are not Raman active in 2H-MoS_2 [37].The transition to as the 1T phase is caused by electron transfer from intercalated Li, which destabilize the original trigonal prismatic 2H-MoS_2 structure [38].

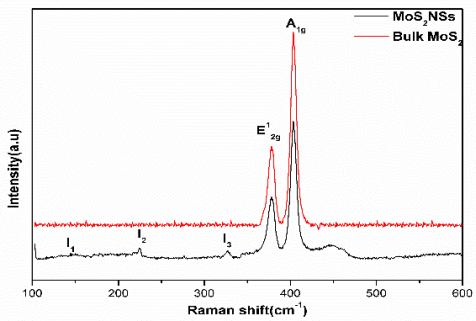

Fig. 3 Raman spectrum of bulk MoS_2 and MoS_2 NSs

3.2 Electrochemical Performance

The electrochemical performances of the as-prepared electrodes were first investigated in a three-electrode system by cyclic voltammetry (CV) and galvanostatic charge-discharge (GCD) tests. Meanwhile, the electrochemical measurements were achieved in 1 M KCl electrolyte solution. Fig. 4(a) shows the CV curves of the Bulk MoS_2, MoS_2 NSs and stainless-steel current collector electrodes at a scan rate of 20 mVs^{-1}. The MoS_2 NS curves present a pair of redox peaks, which states pseudocapacitance features. By comparison, one can find that the area surrounded by the CV curve of MoS_2 NSs electrode is larger than that of bulk MoS_2 and stainless-steel current collector respectively, suggesting a higher specific capacitance. The increased specific capacitance demonstrated superior electrochemical performance which might be due to the exfoliated layers to dynamically expand and intercalate the Li^+ ions.

Fig. 4(b) shows the CV curves of MoS_2 NSs electrode at various scan rates. With the increase of scan rate, the integral area of CV curves and the peak current density are accordingly increased. Meanwhile, a pair of perfectly redox peaks is always retained in all the CV curves. These results indicate the MoS_2 NSs possesses rapid and reversible Faradic behavior and superior rate capability. The specific capacitance as a function of the scan rate is shown in Fig. 4(c). At the scan rate of 1 mVs^{-1}, the specific capacitance values of the Bulk MoS_2 and MoS_2 NSs were 68 and 148 Fg^{-1}, from the cyclic voltammetry measurements, when we increasing the scan rate from 2 mVs^{-1} to 20 mVs^{-1}, around 55% of initial capacitance was retained, respectively.

Further, the supercapacitive behaviors of the prepared electrodes were analyzed using GCD tests. Fig. 4(d) shows the GCD curves of MoS_2 NSs electrodes at the increased current densities from 1 to 5 Ag^{-1}. Fig. 4(e) shows the variation of the specific capacitance value calculated from the charge–discharge curves at different current densities. As can be seen in Fig. 4(d), the charge–discharge curves show a good triangle shape, which indicates the ideal supercapacitive characteristic of MoS_2 NSs electrode. The specific capacitance decays from 148 Fg^{-1} to 80 Fg^{-1} as the current density increases from 1 to 5 Ag^{-1}, which shows the same tendency as CV measurement.

Fig. 4(f) shows cyclic stability of MoS_2 NSs supercapacitors. The cycling measurements of MoS_2 NSs supercapacitors were carried out with cyclic voltammetry at 1 mV s^{-1} for 1000 cycles. The specific capacitance of MoS_2 NSs supercapacitor was decreased from 148 Fg^{-1} at the 1st cycle to 141 Fg^{-1} at the 1000 cycle, with the specific capacitance retention of 94%. This illustrates that MoS_2 NSs based supercapacitor process good stability, lifetime and a high degree of reversibility.

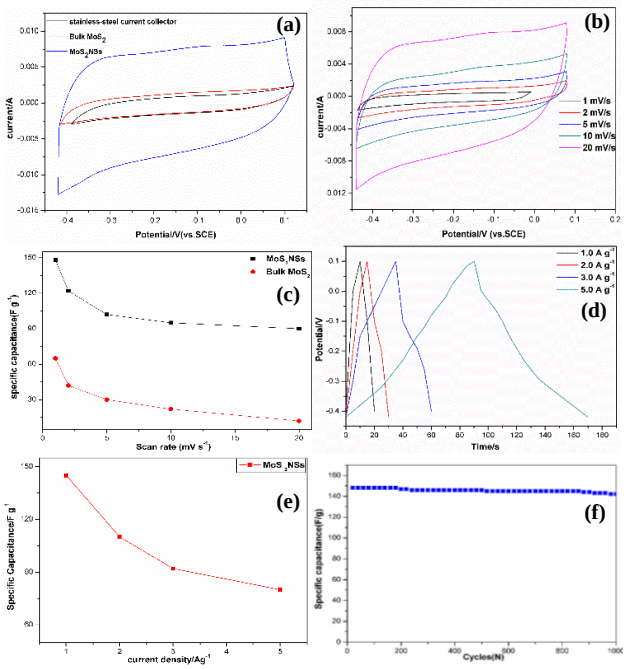

Fig. 4 (a) cyclic voltammetry curves of the bulk MoS_2 and MoS_2 NSs electrodes at a scan rate of 25 mV s^{-1}, (b) CV curves of bulk MoS_2 and MoS_2 NSs electrode at various scan rates, (c) Specific capacitance of bulk MoS_2 and MoS_2 NSs electrodes at different scan rates, (d) Galvanostatic charge/discharge curves of MoS_2 NSs electrodes at different current densities, (e) Specific capacitance of MoS_2 NSs electrodes at various current densities and (f) Cycling performance of MoS2 NSs electrode at 1 mVS^{-1} for 1000 cycles

4. Conclusion

The MoS_2 NSs have been prepared as electrode materials for supercapacitors through a facile and efficient strategy. The morphology and structure of the MoS_2 NSs were analyzed by FESEM, XRD and Raman analysis. Electrochemical measurements indicate that the MoS_2 NSs electrode exhibited a higher specific capacitance (148 Fg^{-1}), as well as a better cyclic stability than the bulk MoS_2 electrode. It is concluded that

https://doi.org/10.30799/jnst.108.18040301

Cite this Article as: K.M. Sarode, D.R. Patil, Metallic 1T phase MoS_2 nanosheets for supercapacitor application, J. Nanosci. Tech. 4(3) (2018) 371–373.

these MoS_2 NSs with excellent electrochemical performance can be very promising for high performance electrode materials in supercapacitors and other energy-storage devices.

References

[1] Y.P. Gao, Z.B. Zhai, K.J. Huang, Y.Y. Zhang, Energy storage applications of biomass-derived carbon materials: batteries and supercapacitors, New J. Chem. 41 (2017) 11456-11470.

[2] L. Wang, Y. Ma, M. Yang, Y. Qi, Titanium plate supported MoS_2 nanosheet arrays for super capacitor application, Appl. Surf. Sci. 396 (2017) 1466-1471.

[3] Y.P. Gao, K.J. Huang, $NiCo_2S_4$ materials for supercapacitor applications, Chem. Asian Jour. 12 (2017) 1969-1984.

[4] L.L. Xing, K.J. Huang, S.X. Cao, H. Pang, Chestnut shell-like $Li_4Ti_5O_{12}$ hollow spheres for high-performance aqueous asymmetric supercapacitors, Chem. Eng. Jour. 332 (2018) 253-259.

[5] Y.P. Gao, K.J. Huang, H.L. Shuai, L. Liu, Synthesis of sphere-feature molybdenum selenide with enhanced electrochemical performance for supercapacitor, Mater. Lett. 209 (2017) 319-322.

[6] L.L. Xing, K.J. Huang, L.X. Fang, Preparation of layered graphene and tungsten oxide hybrids for enhanced performance supercapacitors, Dalton Trans. 45 (2016) 17439-17446.

[7] P. Intawin, F.N. Sayed, K. Pengpat, J. Joyner, C.S. Tiwary, P.M. Ajayan, Bio-derived hierarchical 3D architecture from seeds for supercapacitor application, Jour. Mineral. Metal. Mater. Soc. 69 (2017) 1513-1518.

[8] X. Yang, L. Zhao, J. Lian, Arrays of hierarchical nickel sulfides/MoS_2 nanosheets supported on carbon nanotubes backbone as advanced anode materials for asymmetric supercapacitor, J. Power Source 343 (2017) 373-382.

[9] Y.P. Gao, X. Wu, K.J. Huang, L.L. Xing, Y.Y. Zhang, L. Liu, Two-dimensional transition metal diseleniums for energy storage application: a review of recent developments, Cryst. Eng. Comm. 19 (2017) 404-418.

[10] A.K. Thakur, R.B. Choudhary, M. Majumder, G. Gupta, M.V. Shelke, Enhanced electrochemical performance of polypyrrole coated MoS_2 nanocomposites as electrode material for supercapacitor application, J. Electroanal. Chem. 782 (2016) 278-287.

[11] A.P.P. Alves, R. Koizumi, A. Samanta, L.D. Machado, A.K. Singh, D.S. Galvao, et al., One-step electrodeposited 3D-ternary composite of zirconia nanoparticles, RGO and polypyrrole with enhanced supercapacitor performance, Nano Energy 31 (2017) 225-232.

[12] Y.P. Gao, K.J. Huang, C.X. Zhang, S.S. Song, X.Wu, High-performance symmetric supercapacitor based on flower-like zinc molybdate, J. Alloys Comp. 731 (2018) 1151-1158.

[13] K.W. Qiu, M. Lu, Y.S. Luo, X.W. Du, Engineering hierarchical nanotrees with $CUCO_2O_4$ trunks and NiO branches for high-performance supercapacitors, J. Mater. Chem. A 5 (2017) 5820-5828.

[14] H.S. Hou, C.E. Banks, M.J. Jing, Y. Zhang, X.B. Ji, Carbon quantum dots and their derivative 3D porous carbon frameworks for sodium-ion batteries with ultralong cycle life, Adv. Mater. 27 (2015) 7861-7866.

[15] K. Shiva, H.S.S.R. Matte, H.B. Rajendra, A.J. Bhattacharyya, C.N.R. Rao, Employing synergistic interactions between few-layer WS_2 and reduced graphene oxide to improve lithium storage, cyclability and rate capability of Li-ion batteries, Nano Energy 2 (2013) 787-793.

[16] B. Wang, Y. Xia, G. Wang, Y. Zhou, H. Wang, Core shell MoS_2/C nanospheres embedded in foam-like carbon sheets composite with an interconnected macroporous structure as stable and high-capacity anodes for sodium ion batteries, Chem. Eng. Jour. 309 (2016) 417-425.

[17] B. Chen, E. Liu, T. Cao, F. He, C. Shi, C. He, et al., Controllable graphene incorporation and defect engineering in MoS_2-TiO_2 based composites: towards high-performance lithium-ion batteries anode materials, Nano Energy 33 (2017) 247-256.

[18] T.F. Jaramillo, K.P. Jorgensen, J. Bonde, J.H. Nielsen, S. Horch, I. Chorkendorff, Identification of active edge sites for electrochemical H_2 evolution from MoS_2 nanocatalysts, Sci. 317 (2007) 100-102.

[19] J.Z. Wang, L. Lu, M. Lotya, J.N. Coleman, S.L. Chou, H.K. Liu, et al., Development of MoS_2 CNT composite thin film from layered MoS_2 for lithium batteries, Adv. Energy Mater. 3 (2013) 798–805.

[20] T.M. Masikhwa, M.J. Madito, A. Bello, J.K. Dangbegnon, N. Manyala, High performance asymmetric supercapacitor based on molybdenum disulphide/graphene foam and activated carbon from expanded graphite, J. Colloid Interf. Sci. 488 (2017) 155-165.

[21] S.P. Jose, C.S. Tiwary, S. Kosolwattana, P. Raghavan, L.D. Machado, C. Gautam, T. Prasankumar, J. Joyner, S. Ozden, D.S. Galvao, P.M. Ajayan, Enhanced supercapacitor performance of a 3D architecture tailored using atomically thin rGO–MoS_2 2D sheets, RSC Adv. 6 (2016) 93384-93393.

[22] M.Q. Wen, T. Xiong, Z.G. Zang, W. Wei, X.T. Tang, F. Dong, Synthesis of MoS_2/g-C_3N_4 nanocomposites with enhanced visible-light photocatalytic activity for the removal of nitric oxide (NO), Opt. Express 24 (2016) 10205-10212.

[23] S.J. Deng, Y. Zhong, Y.X. Zeng, Y.D. Wang, Z.J. Yao, F. Yang, et al., Directional construction of vertical nitrogen-doped 1T-2H $MoSe_2$/graphene shell/core nanoflake arrays for efficient hydrogen evolution reaction, Adv. Mater. 29 (2017) 1700748-1700755.

[24] L. She, J. Li, D. Gu, Y. Shi, R. Che, D. Zhao, High-resolution electron microscopy study of mesoporous dichalcogenides and their hydrogen storage properties, Nanotechnol. 22 (2011) 075702-075707.

[25] B. Hinnemann, P.G. Moses, J. Bonde, K.P. Jorgensen, J.H. Nielsen, S. Horch, et al., biomimetic hydrogen evolution: MoS_2 nanoparticles as catalyst for hydrogen evolution, Cheminform. 127 (2005) 5308-5309.

[26] Q.H. Wang, K. Kalantar-Zadeh, A. Kis, J.N. Coleman, M.S. Strano, Electronics and optoelectronics of two-dimensional transition metal dichalcogenides, Nature Nanotechnol. 7 (2012) 699-712.

[27] C. Zhu, X. Mu, P.P.A. van, X. Aken, Y. Yu, J. Maier, Single-layered ultrasmall nanoplates of MoS_2 embedded in carbon nanofibers with excellent electrochemical performance for lithium and sodium storage, Angew. Chem. Inter. Edn. 53 (2014) 2152-2156.

[28] Z. Jian, High yield exfoliation of two-dimensional chalcogenides using sodium naphthalenide, Nature comm. 5 (2014) 2995-3011.

[29] U. Maitra, U. Gupta, M. De, R. Datta, A. Govindaraj, C.N. Rao, highly effective visible-light-induced H, Angew. Chem. Int. Ed. 52 (2013) 13057-13061.

[30] T. Zhang, L.B. Kong, M.C. Liu, Y.H. Dai, K. Yan, B. Hu, et al., Design and preparation of MoO_2/MoS_2 as negative electrode materials for supercapacitors, Mater. Design 112 (2016) 88-96.

[31] G. Eda, H. Yamaguchi, D. Voriy, T. Fujita, M. Chen, Chhowalla, M. Photoluminescence from chemically exfoliated MoS_2, Nano Lett. 11 (2011) 5111-5116.

[32] A. Ramadoss, S.J. Kim, Improved activity of a graphene–TiO_2 hybrid electrode in an electrochemical supercapacitor, Carbon 63 (2013) 434-445.

[33] Y. Liu, Y. Zhao, L.Jiao, J. Chen, A graphene-like MoS_2/graphene nanocomposite as a highperformance anode for lithium ion batteries, J. Mater. Chem. A 2 (2014) 13109-13115.

[34] Z. Zeng, Z. Yin, X. Huang, H. Li, Q. He, G. Lu, et al., Single-layer semiconducting nanosheets: high-yield preparation and device fabrication, Angew. Chem. Int. Ed. 50 (2011) 11093-11097.

[35] D. Yang, S.J. Sandoval, W.M.R. Divigalpitiya, J.C. Irwin, R.F. Frindt, Structure of single-molecular-layer MoS_2, Phys. Rev. B 43 (1991) 12053-12056.

[36] G. Eda, H. Yamaguchi, D. Voiry, T. Fujita, M. Chen, M. Chhowalla, Photoluminescence from chemically exfoliated MoS_2, Nano. Lett. 11 (2011) 5111-5116.

[37] D. Yang, S.J. Sandoval, W.M.R. Divigalpitiya, J.C. Irwin, R.F. Frindt, Structure of single-molecular-layer MoS_2, Phys. Rev. B 43 (1991) 12053- 12056.

[38] M.A. Py, R.R. Haering, Structural destabilization induced by lithium intercalation in MoS_2 and related compound, Can. J. Phys. 61 (1983) 76-84.

https://doi.org/10.30799/jnst.108.18040301

Cite this Article as: K.M. Sarode, D.R. Patil, Metallic 1T phase MoS_2 nanosheets for supercapacitor application, J. Nanosci. Tech. 4(3) (2018) 371–373.